Science Press

ARTICLE

Conductive SrVO$_3$ Powders Synthesized by Sol-Gel Method

Ouyang Linfeng, Yang Xiaojiao, Li Xiaolei, Du Yibo, Lin Zifeng, Liu Ying

College of Materials Science and Engineering, Sichuan University, Chengdu 610065, China

Abstract: Conductive SrVO$_3$ powders were synthesized by sol-gel method combined with subsequent heat treatment. The molar ratio of Sr:V was adjusted during the sol process. The thermal behavior of the gel was analyzed to figure out the calcination temperature in order to get the precursors without residual carbon, and then the gel was reduced in H$_2$ to obtain the final products. The influence of temperature and molar ratio of Sr:V on the morphologies, structures and compositions was researched. The conductivity of the samples was tested by standard dc four-probe technology. The results show that when the molar ratio of Sr:V=1:1.06, the calcination temperature is 500 °C and reduction temperature is 850 °C in H$_2$, the SrVO$_3$ powers without the impurities of residual carbon or vanadium oxides can be obtained. The electrical conductivity of SrVO$_3$ powders reaches 714.3 S/cm, while that of graphite powders is about 500 S/cm.

Key words: SrVO$_3$ powders; sol-gel method; electrical conductivity; thermal behaviour; impurities

---

SrVO$_3$, as one of transition metal oxides with perovskite structure, has attracted much attention due to its excellent ferro-electricity, superconductivity, ferromagnetism and full spin polarization in the conductor[1,2]. SrVO$_3$ was first prepared through solid reactions in 1950s by Kestigian Michael[3] with a cubic perovskite lattice. Its paramagnetic and metallic features at room temperature have been reported[4,5]. Due to the high conductivity, SrVO$_3$ and its derivatives are also competing candidates as the anodes of the solid-oxides-based fuel cells[6]. What's more, the unique cubic perovskite structure brings many unique physical properties to SrVO$_3$, for example, acting as ideal Mott semiconductors[7-9] and transparent conductive oxide[10-12]. Besides, because of the similarity in the 3d^1 electrons of V^{4+} and perovskite copper oxides with newly-reported superconductivity[13], SrVO$_3$ may also have such characteristic as superconductors.

Up to now, the syntheses of SrVO$_3$ are mainly realized from thin films and powders, in which the thin films are generally made through hybrid molecular beam epitaxy (hMBE)[14,15], pulsed laser deposition (PLD)[16,17] and pulsed e-beam deposition (PED)[18,19], while the powders are normally fabricated by the conventional solid state reaction method[4,5]. The SrVO$_3$ powders prepared by the solid state reaction method are calcined at 700 °C for 2 d with intermediate grindings and then reduced several times at 1000 °C in H$_2$ with intermittent grinding and pelleting, and the conductivity of the final products of SrVO$_3$ powders is 41.8 mΩ·cm (23.9 S/cm) at room temperature[4]. It has the disadvantages of long calcination time, high calcination temperature, and large unevenness in structure and composition. The SrVO$_3$ bulk is prepared by spark plasma sintering and has the conductivity of 10^{-5} Ω·m (~1000 S/cm) with bulk density of 95%[5], and the conductivity of SrVO$_3$ products is 7×10^{-4} Ω·cm (~1428 S/cm) fabricated by solid reaction with 65 kb pressure and gold seal in an belt type device[20]. There is a huge gap of conductivity between the SrVO$_3$ powders and SrVO$_3$ bulk, which is not only because of the density but also the purity. Therefore, it is still a challenge to fabricate the SrVO$_3$ powders with good purity and enhancement conductivity by a facile and efficient fabrication method.

Sol-gel method is an excellent candidate to fabricate the SrVO$_3$ powders. It combines the raw materials at an ionic scale in solution, which is beneficial to the homogenization and refinement of components. It can also reduce the reaction temperature and facilitate the preparation process due to the thermal behavior of the complex gel. It has been used to

---

prepare perovskite compounds like $La_{0.8}Sr_{0.2}CoO_3$[21], $Sr(V_{0.5}Mo_{0.5})O_3$[22] and $La_{0.65}Sr_{0.35}MnO_3$[23]. Thus, this work is focused on the fabrication of $SrVO_3$ powders with high purity and good conductivity by a sol-gel method combined with subsequent thermal treatment. The thermal behavior of the complex gel was analyzed and the influence of temperature and molar ratio of Sr: V on the morphologies, structures, components and the electrical conductivity of the $SrVO_3$ powders was also studied.

1 Experiment

$Sr(NO_3)_2$ (Chron, AR, China) and NH_4VO_3 (Chron, AR, China) were used as raw materials of Sr and V. The anhydrous citric acid (Chron, AR, China) was used as complex agent. Then, the three materials deionized water at different stoichiometric ratios, where the molar ratio of citric acid to total metal ion content was 1.1~1.5. The solution was continuously stirred and heated at 80 °C for fully complex to obtain a dark blue transparent sol. With continuous heating and stirring, the sol was transferred to a dark blue gel and then treated in an oven at different temperatures in air for 0.5 h to obtain the precursors. Finally, the precursors were reduced at 850 °C in H_2 for 2 h to fabricate the samples.

The thermal behavior of gel was analyzed by thermo-gravimetric analysis and differential scanning calorimetry (TG-DSC, TA Instruments, Q600 SDT) in air at 800 °C. The structures and phase of samples were characterized by X-ray diffraction (XRD, Shimadzu, 6100) with Cu Kα irradiation (λ= 0.154 06 nm) in the 2θ scan range of 20°~90°. The morphology of the products was collected by transmission electron microscope (TEM, JEOL, JEM-2100F) and search engine marketing (SEM, JEOL, JSM-7800F). Raman (Horiba Jobin-Yvon, LabRAM HR Evolution) spectra were used to determine the type of residual carbon in the sample, and the carbon content was measured by high frequency infrared carbon sulfur analyzer (DEKAI, DK606). The valence state of vanadium was analyzed by X-ray photoelectron spectroscopy (XPS, Thermo Scientific Escalab, 250Xi). The specific surface area and pore diameter of the powders were measured by Brunner-emmet-teller measurements (BET, MICROMERITICS, Micromeritics Gemini VII). The electrical conductivity of the powders was measured at room temperature using a standard dc four-probe technique by pressing the powders at 20 MPa.

2 Results and Discussion

2.1 Thermal behavior of the complex gel

The TG-DSC spectra test of the gel sample with Sr: V=1:1 was conducted in air at 800 °C (as shown in Fig.1). It can be divided into four stages including four major peaks of DSC curve: (1) the first stage with 19% mass loss with an endothermic peak around 110 °C, which can be concluded for the evaporation of the solvent within the gel precursor; (2) a 19.7% mass loss occurs in the second stage with an exothermic peak at 175 °C, which is caused by redox reaction
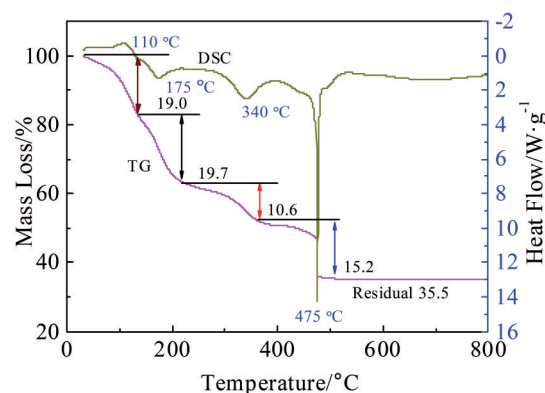

Fig.1 TG-DSC spectra of as-prepared gel precursor

between free citric acid that is not coordinated with metal ions and NO_3^- [24]; (3) the third stage has 10.6% mass loss and an exothermic process at 340 °C, which may be due to the decomposition of the complex to form the corresponding metal oxide; (4) the last stage has 15.2% mass loss due to the severe exothermic reaction with a sharp peak at 475 °C, indicating the combustion of the remaining organic components in the complex[25]. No obvious peaks and mass loss can be found after 475 °C, which means that the thermal decomposition of gel precursor in air has finished over this temperature, and the final sample mass maintains 35.5%. According to the TG-DSC results, the heat treatment temperature is fixed at 200, 350, and 500 °C.

2.2 Influence of temperature on the morphologies and structures

The SEM images of the gel calcined at different temperatures are shown in Fig.2. It can be clearly seen that the morphologies of the samples are typical sheet foam structures by sol-gel. The surface changes significantly as shown in the illustration insets from smooth to porous. When the calcination temperature of the gel is 200 °C, according to the TG-DSC results, the complex has not yet been decomposed at this time, so the surface of the block is smooth as shown in Fig.2a. The complex begins to decompose at 350 °C and the surface becomes porous, as shown in Fig.2b. After calcination at 500 °C, the crystal grains on the surface obviously grow and bond, as shown in Fig.2c.

The corresponding XRD patterns are shown in Fig. 3. Apparently, after the gel precursor is calcined at 200 °C, no obvious characteristic peak appears, indicating that the complex has not been decomposed at this temperature to form a new crystalline product, and some $Sr_2V_2O_7$ characteristic peaks can be observed at 350 °C. When the sample is calcined at 500 °C, the gel precursor is completely decomposed and $Sr_2V_2O_7$ formed (PDF#04-011-5542) with a small amount of V_2O_5 (PDF#97-005-9960) that might be decomposed from the noncomplex NH_4VO_3. Such phenomenon arises from the slightly blocked ionization of citric acid due to the low pH value of the solution, which in turn leads to the unsaturated complex between NH_4VO_3 and citric acid[26,27]. It can be seen
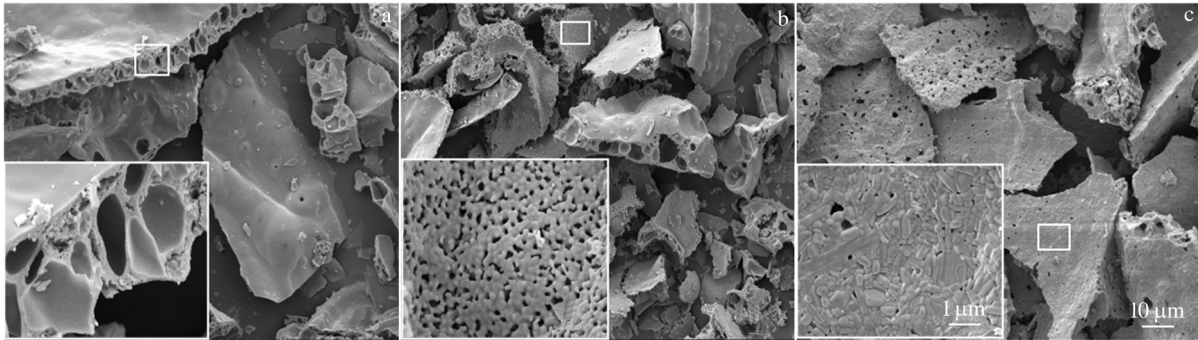
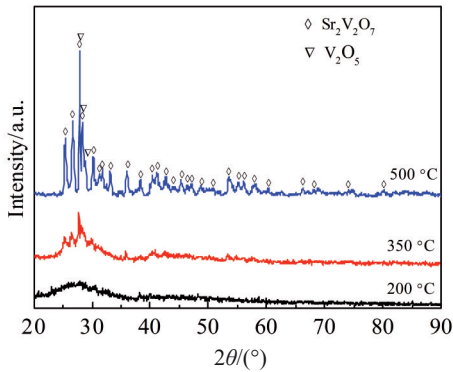Fig.2   SEM images of the gel calcined at different temperatures: (a) 200 °C, (b) 350 °C, and (c) 500 °C

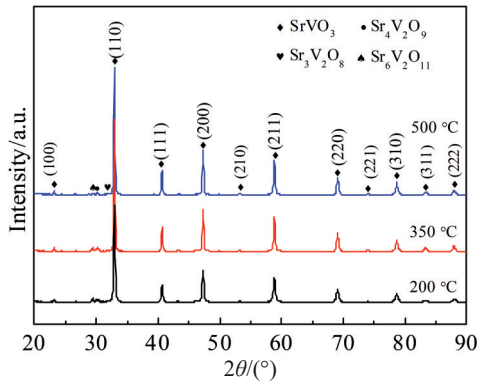Fig.3   XRD patterns of gel precursors calcined at different temperatures in air

Fig.4   XRD patterns of the precursors reduced in H_2 at 850 °C

that the heat treatment of the gel precursor in air will finally reach the valence of V in $Sr_2V_2O_7$ as +5. The powder precursors obtained at different temperatures are reduced in H_2 at 850 °C and the XRD patterns are shown in Fig.4. It is obvious that $SrVO_3$ (PDF#04-007-9076) can be obtained from three different precursors after reduction, but there are some impurities of $Sr_3V_2O_8$, $Sr_4V_2O_9$ and $Sr_6V_2O_{11}$ in the final product, which is because of the insufficient supply of V source.

As shown in Table 1, with the increase of the calcination temperature from 200 °C to 500 °C, the grain size of the reduced samples slightly increases from 35.9 nm to 47.3 nm, and the particle size increases from 5.68 μm to 7.59 μm. On the contrary, the specific surface area of the powder decreases sharply from 60.95 m^2/g to 2.43 m^2/g.

The carbon content of the final product from the precursor calcined at 200 °C is 9.63%. As the calcination temperature increases, the carbon content decreases from 1.46% at 350 °C to 0% at 500 °C. The existence of carbon is due to the calcination of the gel precursor at low temperature, which causes the complex to be incompletely decomposed based on the explanation of TG-DSC results. In addition, as the calcination temperature of the precursor increases, the conductivity of the sample also increases, from 50.1 S/cm (200 °C) to 92.6 S/cm (350 °C), and to 114.5 S/cm (500 °C). That is contributed to the decrease of the content of residual carbon. The Raman spectra in Fig.5 show that when the precursors are calcined at lower temperatures (200 and 350 °C), there are two obvious peaks in the Raman spectrum: D band and G band, in which D band is about 1364 cm^{-1} and G band is

Table 1   The information of products after reduction prepared with different calcination temperature

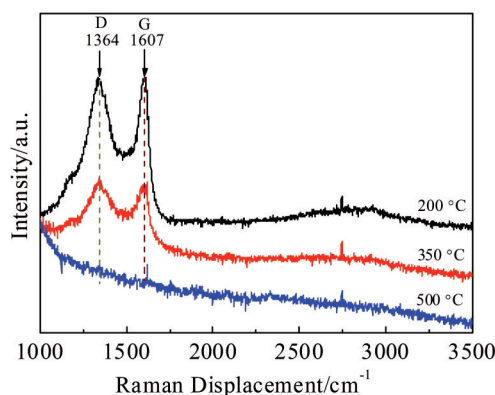| Characterization	Precursor temperature/°C		
	200	350	500
Main phase	$SrVO_3$	$SrVO_3$	$SrVO_3$
Impurity	$Sr_4V_2O_9$, $Sr_6V_2O_{11}$	$Sr_4V_2O_9$, $Sr_6V_2O_{11}$	$Sr_4V_2O_9$, $Sr_6V_2O_{11}$, $Sr_3V_2O_8$
Grain size/nm	35.9	41.9	47.3
Particle size/μm	5.68	7.32	7.59
BET/$m^2 \cdot g^{-1}$	60.95	8.46	2.43
Carbon content/%	9.63	1.46	0
Conductivity/$S \cdot cm^{-1}$	50.1	92.6	114.5

Fig.5 Raman spectra of the samples reduced in H_2 at 850 ℃

located at 1607 cm^{-1}. The intensity ratio of the two bands (I_D/I_G) is about 1.87, which indicates that the precursor heated at a lower temperature will result in amorphous carbon with a low degree of graphitization[28]. When the calcination temperature is 500 ℃, D or G band disappear in Raman spectra, which indicates that there is no carbon, and this result is consistent with the result that the carbon content is 0% from carbon and sulfur analysis. The TEM image in Fig. 6 displays that amorphous carbon is distributed around the particles. The lattice fringes can be clearly observed in the illustration, and the measured interplanar spacing is 0.19 nm, which corresponds to the (002) crystal plane of $SrVO_3$.

Based on the results discussed above, the calcination temperature for the precursors is fixed at 500 ℃ to avoid the residual carbon. But there are still other impurities of $Sr_3V_2O_8$, $Sr_4V_2O_9$ and $Sr_6V_2O_{11}$ in the final product of $SrVO_3$ powders, which is because of the insufficient supply of V source. So regarding on the influences of the amount of initial agents and residual carbon, the amount of $Sr(NO_3)_2$ and NH_4VO_3 is adjusted to tune the molar ratio of Sr:V from 1:1 to 1:1.08 by increasing the V source in the gel, and then calcined at 500 ℃ followed by the reduction in H_2 at 850 ℃.

2.3 Adjusting the molar ratio of Sr:V for pure $SrVO_3$

Fig. 7 shows the XRD patterns of the samples obtained from different molar ratio of Sr:V from 1:1.00 to 1:1.08. All the samples are maily composed of $SrVO_3$ (PDF#04-007-9076)
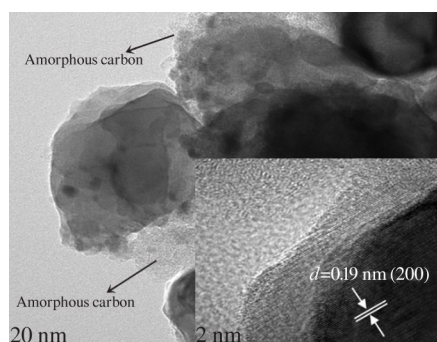

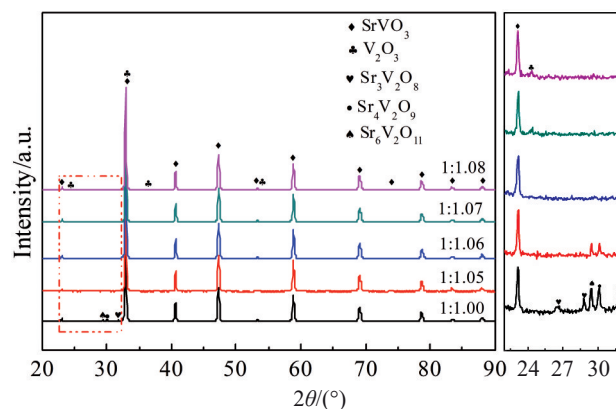Fig.6 TEM image of powders reduced by precursor prepared at 200 ℃

Fig.7 XRD patterns of the samples prepared with different initiator ratios

that is consistent with of the results of Fig. 4. When the molar ratio of Sr:V is 1:1, the diffraction peaks belonging to the impurities of $Sr_3V_2O_8$ (2θ=26.6°, 28.7°, 31.8°, PDF#04-008-3830), $Sr_4V_2O_9$ (2θ=30.1°, PDF#00-028-1270) and $Sr_6V_2O_{11}$ (2θ=29.4°, PDF#00-041-0383) are detected. These excessive strontium vanadium oxide impurities appear in the final product caused by the insufficient V source as discussed before. As increasing the amount of V source to Sr:V=1:1.05, the impurities decrease but still contain $Sr_4V_2O_9$ and $Sr_6V_2O_{11}$. There is no other impurity peaks can be found in the final product when Sr:V=1:1.06. It consists only of pure $SrVO_3$ and the impurities disappear completely. When the Sr:V increases to 1:1.07, more V sources are provided, the diffraction peaks appearing at 2θ=24.3°, 33.0°, 36.2°, 53.9° are identified as the characteristic peaks of V_2O_3 (PDF#04-008-3830) corresponding to the crystal faces of (012), (104), (110) and (116), respectively. Its proportion increases along with the addition of Sr:V=1:1.08, which is due to the increasing V_2O_5 in the gel precursor due to the increase in the amount of NH_4VO_3. By adjusting the molar ratio of Sr:V precisely, the $SrVO_3$ powders without impurities can be obtained.

2.4 Characterization and conductivity of $SrVO_3$ powders

The SEM images in Fig. 8a and 8b display the morphologies of as-prepared $SrVO_3$ as a foam-like frame structure consisting of irregularly connected particles with many loose holes. EDS results show that Sr, V and O are uniformly distributed in the powders, as shown in Fig. 8c~8e. The TEM image in Fig. 8f displays an irregular arrangement of as-prepared $SrVO_3$ particles which are nearly within the nano scale without amorphous carbon. Fig. 8g presents the lattice resolution TEM image of the $SrVO_3$ structure at the edge of the $SrVO_3$ particle in Fig. 8f. The lattice spacing is measured to be 0.27 nm, which corresponds well to the (110) crystal plane, and FFT pattern in Fig. 8h clearly agrees with the standard lattice features of $SrVO_3$ (PDF#04-007-9076).

The O 1s-V 2p spectra in Fig. 9 indicate that vanadium ions exist in two oxidation states. These binding energy value corresponds to the V^{4+} (516.3 and 523.2 eV) and V^{5+} (517.2 and 524.1 eV) states and is consistent with the reported
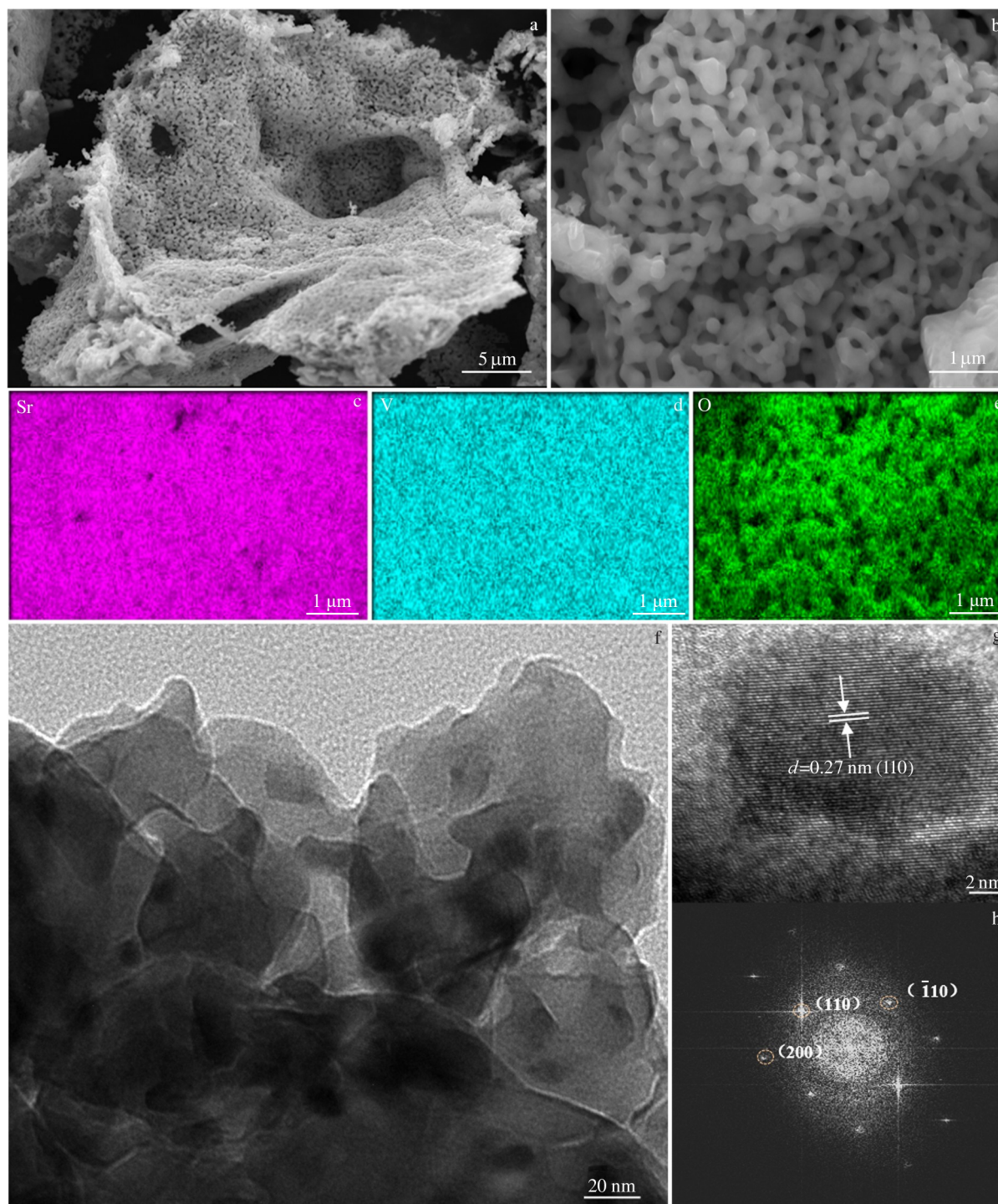
Fig.8　SEM morphologies (a, b) and EDS element mappings of Sr (c), V (d) and O (e) of SrVO$_3$ powders; TEM image (f), HRTEM image (g) and FFT pattern (h) of as-synthesized SrVO$_3$

results[29]. The appearance of V^{5+} is because the surface of SrVO$_3$ is very sensitive to oxygen, which will cause the V^{4+} on the surface to be oxidized to V^{5+}[30].

Fig.10 shows the conductivity of graphite powders and the samples prepared with different Sr∶V ratios. When the molar of Sr∶V=1∶1, the conductivity of the sample containing the impurities of Sr$_3$V$_2$O$_8$, Sr$_4$V$_2$O$_9$ and Sr$_6$V$_2$O$_{11}$ is 114.5 S/cm, which is just 22.9% of the conductivity of graphite powders

(500 S/cm, tested in the same way). With increasing the molar ratio of Sr∶V from 1∶1.05 to 1∶1.06, the conductivity increases from 334.4 S/cm to 714.3 S/cm. It is almost 1.5 times higher than that of graphite powders, and the SrVO$_3$ powders without any impurities indicate excellent metallic properties. In addition, for the samples with the impurities of V$_2$O$_3$ (Sr∶V= 1∶1.07 and 1∶1.08), their electric conductivity is 574.7 and 544.4 S/cm, respectively, much higher than that of the samples
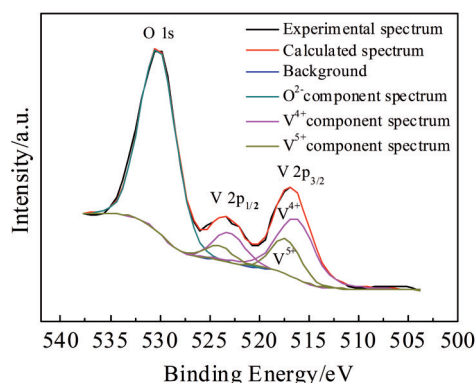
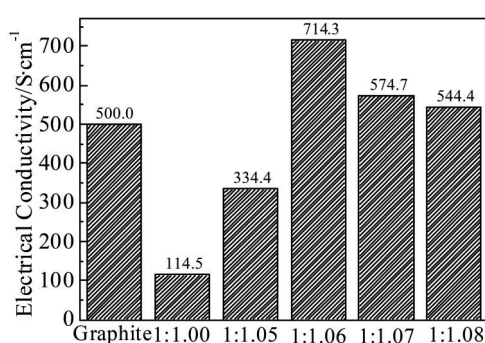Fig.9   O 1s-V 2p XPS spectra of as-synthesized SrVO$_3$ powders

Fig.10   Electrical conductivity of as-synthesized SrVO$_3$ powders

with impurities of strontium vanadium oxides (Sr: V=1: 1.00 and 1: 1.05). It might be concluded that the presence of impurities greatly affect the electrical conductivity of the powders, and the effect of strontium vanadium oxides is higher than that of V$_2$O$_3$. Tuning the molar ratio of Sr: V can obtain the SrVO$_3$ powders without any impurities, and thus the powders possess good purity and excellent conductivity of 714.3 S/cm.

3 Conclusions

1) SrVO$_3$ powders were synthesized by sol-gel method combined with thermal treatment. The thermal treatment influences the morphology, structure and residual carbon content of the precursor powders. The gel precursor is fully decomposed to form Sr$_2$V$_2$O$_7$ and V$_2$O$_5$ at 500 °C in air without any residual carbon.

2) By adjusting the molar ratio of Sr:V precisely to 1:1.06, the final product is reduced, and the SrVO$_3$ powders with good purity and excellent conductivity can be fabricated. The V2p XPS spectrum of as-prepared SrVO$_3$ powders display the dominant existence of V^{5+} and V^{4+}, and the SEM images show a foam-like frame structure consisting of irregularly connected particles with many loose holes. The conductivity of the SrVO$_3$ powders is 714 S/cm, and the presence of impurities greatly affects the conductivity of the powder.

References

1   Zubko P, Gariglio S, Gabay M *et al. Annual Review of Condensed Matter Physics*[J], 2011, 2(1): 141

2   Chakhalian J, Freeland J W, Millis A J *et al. Reviews of Modern Physics*[J], 2014, 86(4): 1189

3   Kestigian M, Dickinson J G, Ward R. *Journal of the American Chemical Society*[J], 1957, 79(21): 5598

4   Lan Y C, Chen X L, He M. *Journal of Alloys and Compounds*[J], 2003, 354(1): 59

5   Maekawa T, Kurosaki K, Yamanaka S. *Journal of Alloys and Compounds*[J], 2006, 426(1): 46

6   Yaremchenko A A, Brinkmann B, Janssen R *et al. Solid State Ionics*[J], 2013, 247-248: 86

7   Oka H, Okada Y, Kaminaga K *et al. Applied Physics Letters*[J], 2020, 117(5): 51 603

8   Wang J, Gauquelin N, Huijben M *et al. Applied Physics Letters*[J], 2020, 117(5): 133 105

9   Itoh M, Shikano M, Kawaji H *et al. Solid State Communications*[J], 1991, 80(8): 545

10   Zhang L, Zhou Y, Guo L *et al. Nature Materials*[J], 2016, 15(2): 204

11   Poeppelmeier K R, Rondinelli J M. *Nature Materials*[J], 2016, 15(2): 132

12   Mirjolet M, Vasili H B, López-Conesa L *et al. Advanced Functional Materials*[J], 2019, 29(37): 1 904 238

13   Bednorz J G, Müller K A. *Zeitschrift für Physik B Condensed Matter*[J], 1986, 64(2): 189

14   Moyer J A, Eaton C, Engel-Herbert R. *Advanced Materials*[J], 2013, 25(26): 3578

15   Brahlek M, Zhang L, Eaton C *et al. Applied Physics Letters*[J], 2015, 107(14): 143 108

16   Sheets W C, Mercey B, Prellier W. *Applied Physics Letters*[J], 2007, 91(19): 192 102

17   Bérini B, Demange V, Bouttemy M *et al. Advanced Materials Interfaces*[J], 2016, 3(18): 1 600 274

18   Gu M, Wolf S A, Lu J. *Applied Physics Letters*[J], 2013, 103(22): 223 110

19   Gu M, Wolf S A, Lu J. *Applied Physics Letters*[J], 2014, 1(7): 1 300 126

20   Patrick, Dougier, John C C *et al. Journal of Solid State Chemistry*[J], 1975, 14(3): 247

21   Wu Yinlin, Wang Ling, Zhao Haiyan *et al. Rare Metal Materials and Engineering*[J], 2007, 36(S2): 145 (in Chinese)

22   Aguadero A, Calle C de la, Pérez-Coll D *et al. Fuel Cells*[J], 2015, 11(1): 44

23   Qiao Liang, Xu Tiantian, Cai Wei *et al. Rare Metal Materials and Engineering*[J], 2010, 39(2): 343 (in Chinese)

24   Sivakumar P, Ramesh R, Ramanand A *et al. Materials Research Bulletin*[J], 2011, 46(12): 2204

25   Xu Q, Chen S, Chen W *et al. Materials Chemistry and Physics*

[J], 2005, 90(1): 111

26　Biedunkiewicz A, Gabriel U, Figiel P *et al. Journal of Thermal Analysis and Calorimetry*[J], 2012, 108(3): 965

27　Liu Junliang, Zhang Wei, Guo Cuijing *et al. Journal of Alloys and Compounds* [J], 2009, 479(1): 863

28　Ferrari A C, Robertson J, Ferrari A C *et al. Philosophical Transactions of the Royal Society of London. Series A:* *Mathematical, Physical and Engineering Sciences*[J], 2004, 362(1824): 2477

29　Demeter M, Neumann M, Reichelt W. *Surface Science*[J], 2000, 454-456: 454

30　Mendialdua J, Casanova R, Barbaux Y. *Journal of Electron Spectroscopy and Related Phenomena*[J], 1995, 71(3): 249

溶胶-凝胶法合成导电SrVO$_3$粉末

欧阳林峰，杨晓娇，李小磊，杜义波，林紫峰，刘　颖

(四川大学 材料科学与工程学院，四川 成都 610065)

摘　要：通过溶胶-凝胶法结合热处理合成了导电SrVO$_3$粉末。在溶胶配制过程，对Sr:V摩尔比进行精确调控，再通过对凝胶热分解行为的表征，确定其煅烧温度和除去残余碳，从而获得前驱体粉末，再将其在H$_2$中还原以获得最终产物。研究了煅烧温度、Sr:V摩尔比对产物形貌、结构和组成的影响，并采用标准直流四探针技术对样品的电导率进行测试。结果表明，当Sr:V摩尔比为1:1.06，煅烧温度500 ℃，再在850 ℃氢气还原，可以制备没有残余碳或钒的氧化物杂质的单相SrVO$_3$粉末。SrVO$_3$粉末的电导率达到714.3 S/cm，比石墨粉末的电导率（500 S/cm）高。

关键词：SrVO$_3$粉末；溶胶凝胶法；电导率；热行为；杂质